

Aqueous solutions of acrylamide–acrylic acid copolymers: stability in the presence of alkaline earth cations

J. François*, N. D. Truong, G. Medjahdi and M. M. Mestdaght

Laboratoire de Recherches sur le Matériaux Polymizes, CNRS/UPPA 2, rue de President Angot, 64000 PAU, France
 (Revised 5 February 1997)

The interactions between acrylamide–acrylic acid copolymers and alkaline earth cations were studied by many different techniques, as functions of various parameters: composition of the copolymer and distribution of the acrylic units along the chain; pH; temperature; ionic strength. In a first step, the phase diagrams were established and reveal ranges of polymer and salt concentrations where phase separation occurs. In a second series of experiments, the change in the chain conformation and the aggregation phenomena were investigated by viscosimetry and light scattering. It sorts out that at low enough polymer and salt concentrations (inside the solubility domain), it is possible to get a variation of the intrinsic viscosity of the polymer as a function of calcium concentration and charge parameter of the polymer consistent with previous literature results obtained in the presence of sodium if a binding term depending on the nature of the ion is taken into account. At higher polymer and calcium concentration, high Huggins constants and large increases of scattered intensity reveal the formation of aggregates, which are attributed to intermolecular bridges. The third series of experiments (conductimetry and densimetry) were carried out to characterize the ion–polyion interactions. Finally, the phase separation is discussed in light of the other results, using some simple association models. © 1997 Elsevier Science Ltd.

(Keywords: aqueous solutions; acrylamide–acrylic acid copolymers; alkaline earth cations)

INTRODUCTION

The changes in the conformation of polyelectrolytes with the ionic strength are not rather well understood¹. On the other hand, the precipitation and gelation phenomena induced by the presence of multivalent counterions in polyelectrolyte solutions have been the object of few theoretical predictions, and there is a lack of reliable data on the phase diagrams of such systems. This is due to the specificity of the ion–polyion interactions. Nevertheless, this problem has been investigated in the years since 1960 by several authors^{2–8}. A set of experimental studies about the stability of the sodium polyacrylate (PAA) towards alkaline earth cations led Ikegami and Imai⁵ to consider two main types of phase separation, so-called:

Type H: where H means that a high salt concentration is required to induce the polymer precipitation. Flory⁹ has developed a model which takes into account the decrease of the electrostatic free energy when the ionic strength of the medium increases. The critical salt concentration C_s^* at the phase separation is expected to be independent of the polymer concentration C_p and increasing function of the temperature. The system solubilizes by heating.

Type L: where the precipitation is observed for low

values of C_s^* corresponding to the stoichiometry with respect to the number of charged groups belonging to the polymer (for example, one Ca^{2+} per COO^- for PAA). In this case, C_s^* does vary with temperature, and is proportional to C_p .

These two types of phase separation describe extreme behaviours. Type H is observed when the specific interactions between the ions and the polyions can be neglected, for example in the case of very weakly charged polyelectrolytes in the presence of multivalent counterions⁵ or in the case of strongly charged polyelectrolytes in the presence of monovalent counterions¹⁰. The second type describes the behaviour of strongly charged polymers which specifically interact with counterions^{2–8}.

In fact, it is well known that a wide range of behaviours can be observed according to the charge of the polyion, the pH, the temperature, the mean ionic strength and the nature of the counterions. Moreover, some cations, particularly ionic species derived from aluminium, chromium and iron are able to induce not only a phase separation but also gelation in aqueous solutions of synthetic polyelectrolytes^{11–18}. It must be noted that the aqueous solutions of natural polycarboxylates such as pectates and alginates can gelify by addition of alkaline earth cations^{19–20}.

We have undertaken a systematic study of the phase separation and gelation of acrylamide–acrylic acid copolymers (AM–AA) in the presence of different cations^{11–16,21–24}. In the case of polyelectrolytes interactions

* To whom correspondence should be addressed

† Present address: Unité de Chimie des Interfaces, Place Croix du Sud 2/18, 1348 Louvain-La-Neuve, Belgium

Table 1 Characteristics of the polymer samples: τ is the fraction of acrylic acid; MMM and AAA are the fractions of acrylamide and acrylic acid triads respectively

	τ	AAA	MMM	ξ for $\alpha = 1$
AD10	0.015	-	-	0.04
AD17	0.07	-	0.81	0.202
AD27	0.17	-	0.65	0.49
AD37	0.27	0.02	0.48	0.78
AD60	0.36	0.34	0.43	1.04
H1	0.17	-	0.5	0.49
H2	0.30	-	0.2	0.867
H3	0.36	-	0.08	1.04
H4	0.50	0.02	0	1.44

with alkaline earth cations, some preliminary results have already been published^{22,23}, showing interesting behaviours with intermediate features between H and L types of precipitation that is to say that precipitation occurs on heating the system, redissolution appears in excess of salt, and the samples prepared by alkaline hydrolysis (samples H) and the copolymerization (AD samples) behave differently. These samples mainly differ in the distribution of the monomers along the chain, which can be characterized by nuclear magnetic resonance (n.m.r.)²⁵. The fractions of triads MMM and AAA are much higher in the case of copolymers. It is indeed well known that alkaline hydrolysis obeys an auto-retarded kinetics, and leads to polymers where the carboxylate groups tend to be isolated along the chain²⁵⁻²⁹. On the other hand, and according to the pH of the reaction, the copolymers are more or less blocky. This block distribution corresponds to the presence along the chain of strongly charged parts which could affect the cation binding. More recently, similar types of phase diagrams have been described for other systems³⁰ and several theoretical approaches are now in progress³¹⁻³³. This strengthens the interest for this kind of studies.

This paper gives a complete description of the influence of alkaline earth cations on the stability of the AM-AA copolymers in aqueous solutions under various conditions of pH, ionic strength and temperature. The effect of the molecular weight has been verified. The ion-polyion interactions are studied by viscosimetry, conductimetry, densimetry and light scattering. A rough model based upon simple association equilibrium laws is proposed in order to explain the phase separation through the theoretical approaches developed by Axelos *et al.*³³ and Wittmer *et al.*³².

EXPERIMENTAL

Samples

Two series of AM-AA copolymers were used in this study:

- a series obtained by alkaline hydrolysis of a polyacrylamide sample (PAM AD10) supplied by Rhone-Poulenc Ind., and prepared by photopolymerization³⁴ (samples H1 to H4);
- a series of copolymers obtained by direct photocopolymerization of acrylamide and acrylic acid (Rhone-Poulenc Ind.): AD17, AD27, AD37, AD60.

All these samples were carefully characterized by ¹³C and ¹H n.m.r., elemental analysis and potentiometric titration²⁵. The values of the average molar fraction τ , of acrylic acid and the fraction of acrylate (AAA) and

acrylamide (MMM) triads are given in *Table 1*. The molecular weight determined by light scattering was found to be around 5×10^6 daltons for all the samples.

In order to investigate the influence of the molecular weight, some of the samples were degraded by ultrasonic absorption by using a generator Mullard 3100 (power ranging from 6 to 16 W) in aqueous solutions (0.5 M NaCl, polymer concentration $c_p = 5 \times 10^{-3}$ g ml⁻¹).

The series H was only used under the form of sodium salt. The copolymers of the AD series are available as sodium salts; they were also purified by precipitation in ethanol-methanol mixtures and a part of them was acidified by stirring their aqueous solutions with an excess of ionic exchangers, again precipitated and then dried under vacuum at 40°C. Some acid samples were neutralized by calcium hydroxide in order to obtain calcium salts. The polymer solutions were prepared at least 48 h before experiments, and homogenized by gentle stirring at room temperature.

These polymers are characterized by their average dimensionless charge density parameter ξ given by^{35,36}:

$$\xi = \left(\frac{e^2}{\epsilon k T} \right) / b \quad (1)$$

where the numerator is the Bjerrum length (7.14 Å in water at 25°C) and b which is the average spacing between two charges assuming a statistical distribution of the charges is calculated by $b = 2.79/\alpha\tau$ (α being the ionization degree of the carboxylate groups).

Methods

Turbidimetry. Weighted quantities of salts, under the form of dry powder, were successively added in polymer solutions and the turbidity was measured with a spectrophotometer Shimadzu UV240 at 700 nm. We have verified that the addition of the salt, under the form of a solution, lead to the same results.

Viscosimetry. Two viscometers were used:

- an automatic capillary viscosimeter³⁷ with an average shear rate of about 1500 s⁻¹. In most cases, this does not correspond to a Newtonian behaviour of the solutions studied.
- a low shear viscosimeter from Contraves (LS30) equipped with the 1T1T device.

Both apparatus were thermostated at $\pm 0.05^\circ\text{C}$ for $20^\circ\text{C} < T < 40^\circ\text{C}$ and at $\pm 0.1^\circ\text{C}$ for $T > 40^\circ\text{C}$.

Densimetry. An automatic densimeter of the Kratky type and equipped with a home-built cell was used to determine the specific volume of the solutions³⁸. The accuracy on the density measurements is $\pm 5 \times 10^{-6}$ g ml⁻¹ when the temperature is regulated at $\pm 0.01^\circ\text{C}$.

Conductimetry. The conductivity was measured with an automatic B221 A Wayne Kerr bridge at 1592 Hz by using a Tacussel cell (constant = 1 cm⁻¹). The measurements were made as for turbidimetry after each addition of dry salt. The equilibrium was reached after approximately 15 nm. The vessel was thermostated at $\pm 0.1^\circ\text{C}$.

Light scattering. Light scattering measurements were performed with a home-built apparatus³⁹ of the Scheibling-Wippler type in a scattering angle range between 30° and 150°.

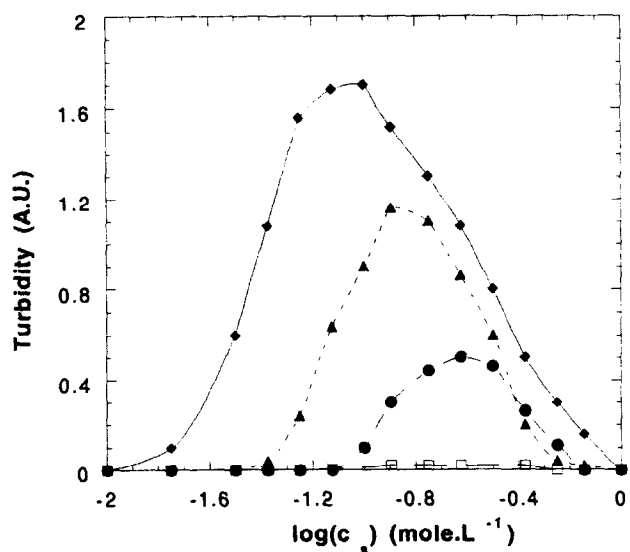


Figure 1 Variation of the turbidity of a solution of polymer H3 as a function of CaCl_2 concentration, for different concentrations of NaCl: $[\text{NaCl}] = 0 \text{ mol l}^{-1}$ (\blacklozenge), $[\text{NaCl}] = 0.05 \text{ mol l}^{-1}$ (\blacktriangle), $[\text{NaCl}] = 0.1 \text{ mol l}^{-1}$ (\bullet) $[\text{NaCl}] = 1 \text{ mol l}^{-1}$ (\square)

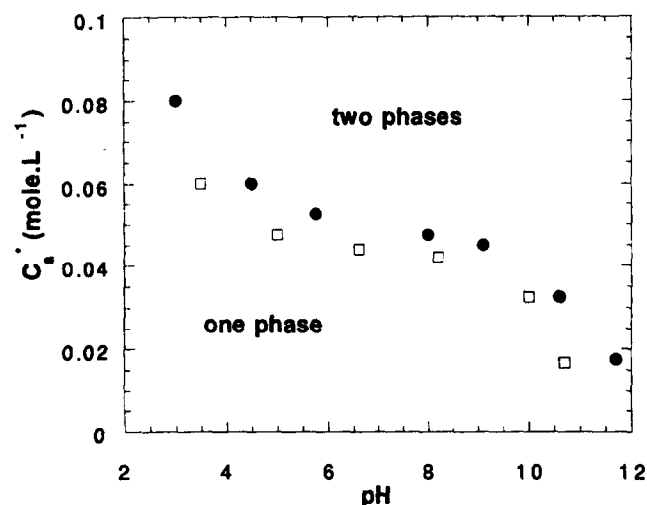


Figure 2 Critical salt concentrations C_s^* as a function of pH when it is adjusted with NaOH (\bullet) or $\text{Ca}(\text{OH})_2$ (\square) for AD60 polymer ($C_p = 10^{-3} \text{ g mol}^{-1}$)

Free salt polymer solutions were prepared at a given polymer concentration and carefully cleaned by filtration and ultracentrifugation at 15000 rpm for 4 h. On the other hand, a concentrated calcium chloride (CaCl_2) solution was also centrifuged and small aliquots were added in the polymer solution contained in the light scattering cell. The scattering intensity was recorded as a function of time after each salt addition.

RESULTS

Phase diagrams

Typical turbidity curves were obtained (Figure 1), by adding chloride salt to the polymer solution, as done previously. Two critical concentrations can be determined:

- the lower one, C_s^* , at which the turbidity abruptly increases. It corresponds to the onset of the polymer precipitation.

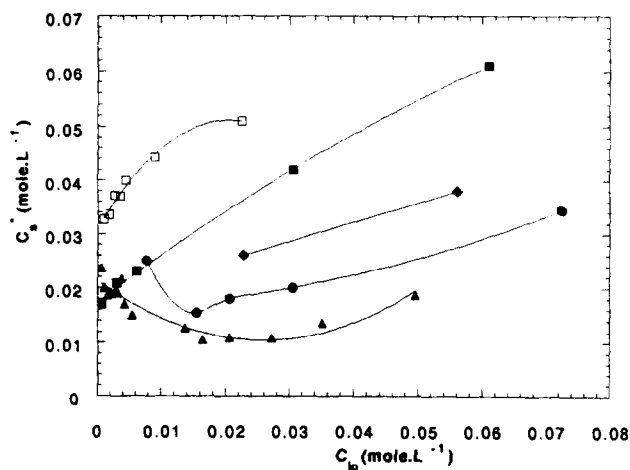


Figure 3 Variation of C_s^* as a function of C_{ip} for polymers: H3 (\square); H4 (\blacksquare); AD27 (\blacklozenge); AD37 (\bullet); AD60 (\blacktriangle)

- the higher one, C_s^{**} , at which the turbidity recovers its initial value (free salt solution) and which indicates the polymer redissolution. As later discussed this unexpected behaviour has already been described^{22,23,40} and also observed in the cases of sodium polyacrylate in the presence of sodium iodide⁴¹ and of polystyrene sulfonate in the presence of trivalent cations³¹.

Salts of alkaline metals. In the absence of salt, all the samples are insoluble in water at $\text{pH} < 3$.

Under their acid form and with increasing amount of NaCl, the onset of precipitation, C_s^* is very high (around 1 M) and increases upon heating. This behaviour is close to a precipitation of type H and reflects the competition between the proton and the Na^+ ions in their affinity for the carboxylate groups.

No phase separation is observed with these polymers when taken under their sodium salt form (pH around 8) if an excess (up to 6 N) of alkaline halides (NaCl, NaBr, KCl) is added. Nevertheless, the co-ion seems to have some influence since AD60 solutions become turbid for a concentration of sodium fluoride higher than 0.8 M. Kagawa and Fuoss⁴¹ have also pointed out that potassium iodide has a much higher salting out effect on PAA than KCl.

Salts of alkaline earth metals. (i) *pH effect:* Figure 2 represents the evolution of the C_s^* value for AD60 in the presence of calcium chloride for solutions neutralized at various pH with sodium or calcium hydroxides.

At $\text{pH} > 12$, the precipitation of the calcium hydroxide occurs. At lower pH, C_s^* decreases when the pH increases. The behaviour is different from that already described for PAA or polymethacrylic acid (PMA) in the presence of copper. In these cases, the curves $C_s^* = f(\text{pH})$ pass through a maximum at $\text{pH} 5^{42,43}$. A given mixture of polymer-copper successively phase separates and becomes again homogeneous and transparent with pH increases. (ii) *Effect of the ionic strength.* In Figure 1, the turbidity is plotted as a function of CaCl_2 concentration for various constant concentrations of NaCl. By addition of NaCl in a two phase system, one recovers an homogeneous solution. For a H sample, the presence of NaCl improves the polymer solubility since C_s^* is shifted towards higher values and C_s^{**} towards lower values. Moreover, the maximum of

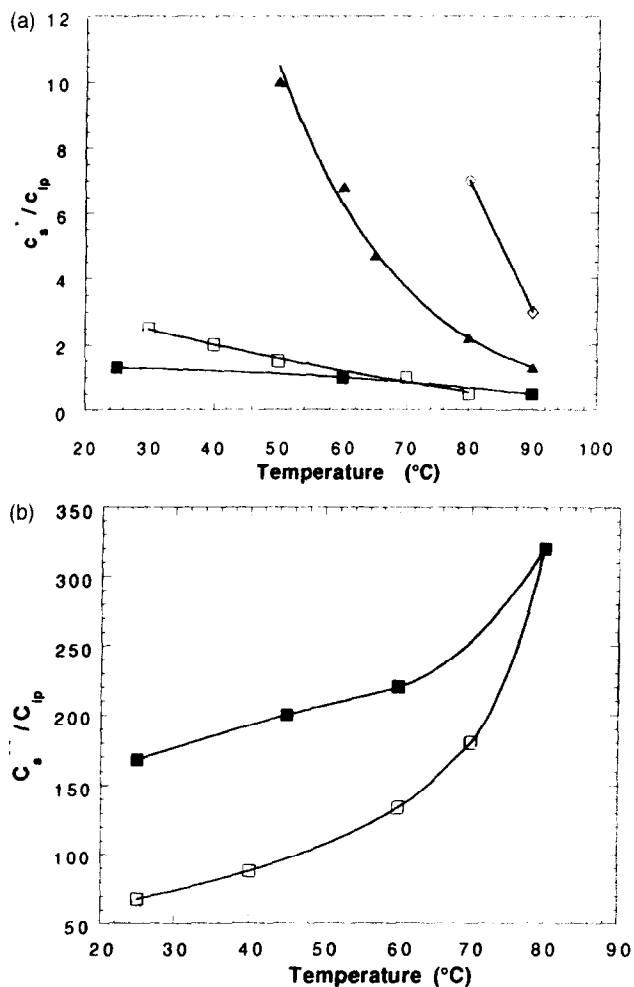


Figure 4 Variations of $R^* = C_s^*/C_{ip}$ (a) and $R^{**} = C_s^{**}/C_{ip}$ (b) as a function of temperature; in (a): AD17 (\diamond); AD27 (\blacktriangle); AD60 (\blacksquare); H4 (\square); in (b) H4 (\square); AD60 (\blacksquare)

turbidity decreases: for 1 M NaCl the precipitation phenomenon is completely hindered by NaCl. The same behaviour is qualitatively observed with the AD samples, but the results show a lower solubility of AD samples with respect to the H ones. (iii) *Influence of the linear charge density and concentration of the polymer.* Figure 3 gives the variations of C_s^* as a function of C_{ip} , which corresponds to the molar concentration of carboxylate groups in the solution, for two samples of type H and three samples of type AD, in pure water at 25°C ($C_{ip} = C_p \cdot 1000 \cdot \alpha \cdot \tau / M_s$, where M_s is the molecular weight of the monomer, and α is taken as equal to 1):

- the stability decreases when the average charge of the polymer increases, for both series of polymers. This is consistent with the variation of C_s^* vs pH underlining the competition of the divalent cation vs the proton for the carboxylate groups.
- however, the behaviour of the two types of polymers differs when considering for the same values of C_p and τ the values of C_s^* : it is much higher for H polymers than for the AD ones. Besides, the shape of the curves is almost linear for H polymers and they tend to exhibit a minimum for AD polymers.

If one considers the ratio $R^* = C_s^*/C_{ip}$ it appears that R^* tends to values close to 0.5 or even lower, when C_p

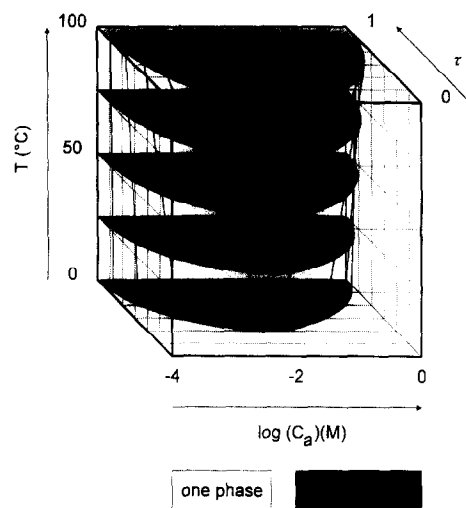


Figure 5 Phase diagrams at constant concentration in polymer

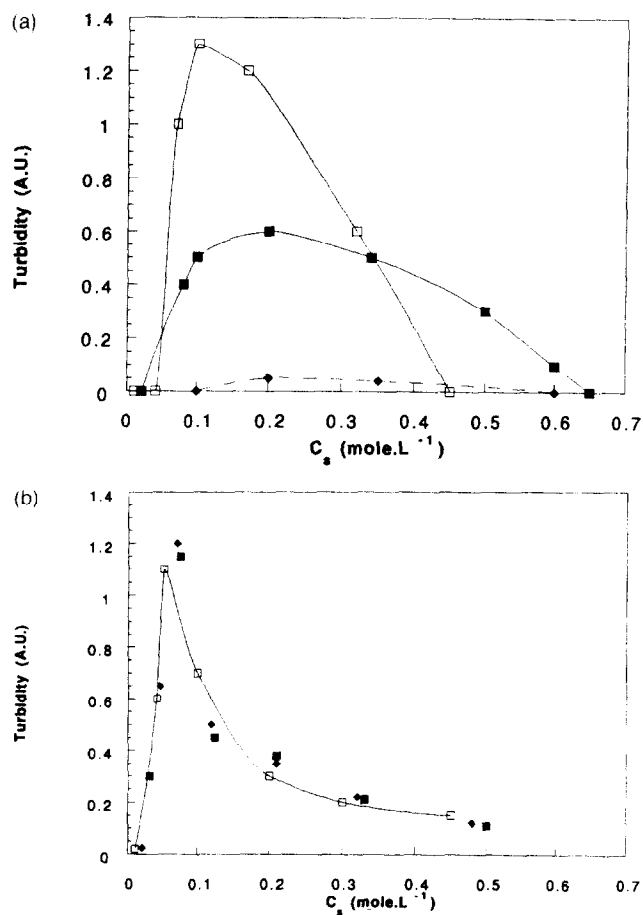


Figure 6 Turbidity curves of samples H3 (a) and AD60 (b), with $\tau = 0.36$, of various molecular weights. (a) $M_w = 5 \times 10^6$ (\square); $M_w = 1 \times 10^6$ (\blacksquare); $M_w = 15.2 \times 10^5$ (\blacklozenge), (b) $M_w = 5 \times 10^6$ (\square); $M_w = 2.8 \times 10^5$ (\blacksquare); $M_w = 1.3 \times 10^5$ (\blacklozenge)

increases. Then, the phase separation of concentrated polymer solutions requires only about one (or less) Ca^{2+} cation per two COO^- groups. This type of curve indicates that the phase separation in our case belongs neither to type L nor to type H, and corresponds to an intermediate behaviour.

The variation of $R^{**} = C_s^{**}/C_{ip}$ with the different parameters also indicates that the stability is improved

by decreasing τ and is higher for H polymers than for AD copolymers (see Figure 4). This explains why this redissolution phenomenon was never observed with PAA. Finally, C_s^{**} is almost independent on C_p and the ratio R^{**} is always very high (50–500). (iv) *Influence of temperature.* Heating homogeneous polymer solutions in the presence of CaCl_2 results in a phase separation. R^* and R^{**} are, respectively, a decreasing and an increasing function of the temperature (Figures 4a and 4b). This means that the solubility of these polymers is strongly affected by heating. At the opposite, as described by Ikegami and Imai⁵, R^* does not depend on T , for the PAA/ Ca^{2+} system. This independence of C_s^* is considered by these authors as characteristic of the precipitation of type L, as well as the low values of C_s^* . We observe with our polymers a precipitation which does not exactly belong to the type L, although the C_s^* values are also very low. Our results are in fact quite consistent with those of Ikegami and Imai⁵ since the absolute values of the average slopes of R^* and R^{**} vs T increase when τ increases. Figure 5 shows the phase diagrams in three dimensions T , C_s , τ , at constant C_p . The surface behind which the phase separation occurs, is obtained from an interpolation procedure of the experimental results. (v) *Effect of the molecular weight.* Figure 6 shows the turbidity curves of samples of various molecular weight obtained by ultrasonic degradation of H3 and AD60 of $\tau = 0.36$. In the case of polymers derived from AD60, phase separation occurs at the same C_s^* values, whatever the M_w . On the other hand, the solubility of H samples seems to be higher when M_w decreases. This result is particularly interesting because it emphasizes the role played by the distribution of the charge on the relative proportion of intra- and inter-molecular binding of the cations. The formation of intermolecular bridges, preponderant in the case of H samples, requires a polymer concentration higher than the critical concentration of chain overlapping C_p^* , which is a decreasing function of M_w . For the lower molecular weight (of about 10^5), the concentration used in the experiment reported in Figure 6 ($10^{-3} \text{ g ml}^{-1}$) is lower than C_p^* and the binding of Ca^{2+} on two carboxylates belonging to two chains cannot occur. On the other hand, if the precipitation is mainly due to the fixation of Ca^{2+} on two adjacent groups along the chain, which is probably the case of AD samples, the onset of phase separation is expected to depend less drastically on molecular weight. (vi) *Effect of the method of preparation of the polymer samples.* The differences in behaviour between samples prepared by alkaline hydrolysis (H samples) and by copolymerization (AD samples) have already been pointed out²², and are well illustrated by several of the results discussed above. Even if these samples have the same molecular weight and polydispersity, they differ in the distribution of the monomers along the chain, as shown in Table 1. The block distribution in the case of AD₃, which is related to the copolymerization parameters^{25,44,45} induces the presence along the chain of strongly charged parts where the cation binding is probably favoured. This well explains the lower solubility of copolymers, if the ion binding is the origin of phase separation. Some potentiometric studies have also shown the role played by the distribution of the monomers^{26,46,47}. (vii) *Effect of the nature of cation.* Table 2 gives the values of C_s^* and C_s^{**} obtained with magnesium, calcium, barium, and manganese chlorides

Table 2 Values of critical salt concentrations at precipitation (C_s^*) and dissolution (C_s^{**}) for the AD60 polymer ($C_p = 10^{-3} \text{ g ml}^{-1}$), in pure water, as a function of the nature of the cation

	Mg^{2+}	Ca^{2+}	Ba^{2+}	Mn^{2+}
C_s^* (mol l ⁻¹)	0.015	0.015	0.009	0.005
C_s^{**} (mol l ⁻¹)	0.57	1.30	1.40	∞

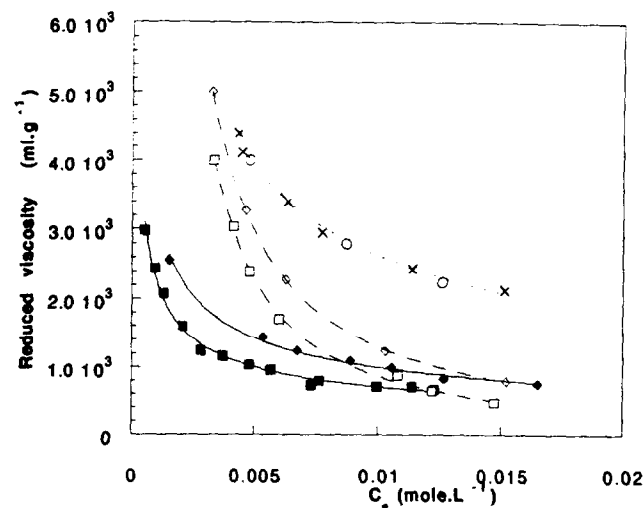


Figure 7 Variation of the reduced viscosity as a function of C_s for the low calcium concentrations: AD60, $C_p = 10^{-3} \text{ g ml}^{-1}$ (■); H3, $C_p = 10^{-5} \text{ g ml}^{-1}$ (◆); AD60, $C_p = 10^{-3} \text{ g ml}^{-1}$ (□); H3, $C_p = 10^{-3} \text{ g ml}^{-1}$ (◇); AD27, $C_p = 10^{-3} \text{ g ml}^{-1}$ (○); H1, $C_p = 10^{-3} \text{ g ml}^{-1}$ (×)

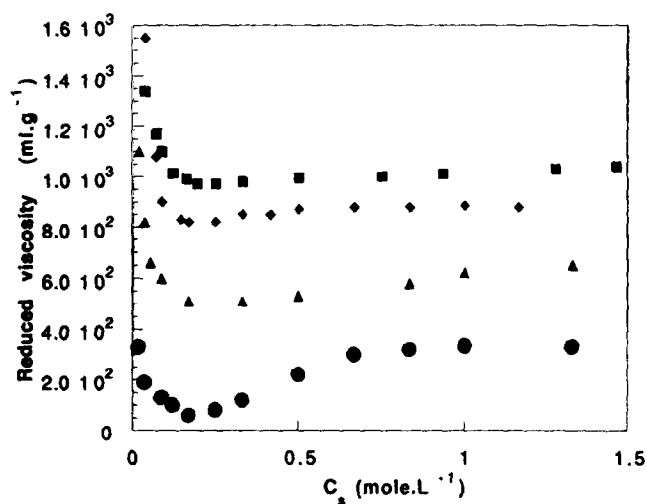
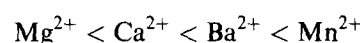
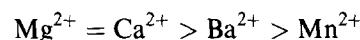


Figure 8 Variation of the reduced viscosity as a function of C_s for the high calcium concentrations at $C_p = 10^{-3} \text{ g ml}^{-1}$: AD17 (■); AD27 (◆); AD37 (▲); AD60 (●)

for AD60 ($C_p = 10^{-3} \text{ g ml}^{-1}$). The following scale of selectivity is obtained for C_s^* and C_s^{**} respectively:



This is in agreement with the observations made by Ikegami and Imai⁵ for partially neutralized polyacrylic acid. When the distance between the charges along the macromolecular chain is low (sodium polyacrylate or polymethacrylate) the selectivity is less pronounced than for the weakly charged polyelectrolyte. In the latter case,

Table 3 Intrinsic viscosity $[\eta]$ and Huggin's constant (K'), at various salt concentrations for AD samples characterized by different charge parameters (ξ): 3A: for NaCl; 3B: for CaCl₂ addition

Sample	C_s (NaCl) mol l ⁻¹	$[\eta]$ (ml g ⁻¹)	K'
(a)			
AD60	0.10	1725	0.34
$\alpha = 0.1$	0.25	1485	0.39
$\xi = 0.104$	0.50	1340	0.35
	0.75	1300	0.42
	1.00	1245	0.48
	2.00	1175	0.49
AD60	0.10	2050	0.35
$\alpha = 0.15$	0.25	1625	0.45
$\xi = 0.153$	0.50	1470	0.41
	0.75	1375	0.46
	1.00	1310	0.47
	2.00	1215	0.53
AD17	0.10	2310	0.29
$\alpha = 1$	0.25	1832	0.35
$\xi = 0.202$	0.50	1563	0.37
	0.75	1460	0.36
	1.00	1382	0.41
	2.00	1265	0.53
AD60	0.10	2605	0.35
$\alpha = 0.25$	0.25	2000	0.43
$\xi = 0.257$	0.50	1682	0.43
	0.75	1545	0.48
	1.00	1453	0.46
	2.00	1297	0.54
AD27	0.10	3842	0.35
$\alpha = 1$	0.25	2710	0.38
$\xi = 0.490$	0.50	2154	0.46
	0.75	1903	0.38
	1.00	1768	0.41
	2.00	1477	0.51
AD37	0.10	4800	0.28
$\alpha = 1$	0.25	3300	0.34
$\xi = 0.780$	0.50	2530	0.36
	0.75	2200	0.42
	1.00	2010	0.35
	2.00	1620	0.45
AD60	0.10	5558	0.32
$\alpha = 1$	0.25	3834	0.39
$\xi = 1.04$	0.50	3021	0.44
	0.75	2443	0.48
	1.00	2203	0.54
	2.00	1730	0.52
(b)			
AD60	0.005	1817	1.04
$\alpha = 0.1$	0.01	1588	1.22
$\xi = 0.104$	0.02	1428	1.05
	0.04	1322	1.12
AD60	0.005	2113	1.11
$\alpha = 0.15$	0.01	1805	1.05
$\xi = 0.153$	0.02	1585	1.04
	0.04	1427	1.21
AD17	0.005	2367	1.03
$\alpha = 1$	0.01	1987	1.45
$\xi = 0.202$	0.02	1702	1.02
	0.04	1518	0.98
AD60	0.005	2658	1.55
$\alpha = 0.25$	0.01	2178	1.68
$\xi = 0.257$	0.02	1850	1.13
	0.04	1604	1.65
AD27	0.005	3684	1.70
$\alpha = 1$	0.01	2923	1.73
$\xi = 0.490$	0.02	2332	1.66
	0.04	1940	1.48

Table 3 Continued

Sample	C_s (NaCl) mol l ⁻¹	$[\eta]$ (ml g ⁻¹)	K'
AD37	0.005	4308	1.71
$\alpha = 1$	0.01	3320	1.10
$\xi = 0.78$	0.02	2617	1.10
	0.04	2133	1.50
AD60	0.005	4638	1.80
$\alpha = 1$	0.01	3529	1.20
$\xi = 1.04$	0.02	2783	1.60
	0.04	2238	1.10

this distance is much higher, and the size of the cation plays a more important role. The transition metal ions induce more easily the polymer precipitation, since C_s^* is lower than for alkaline earth cations⁴⁸.

We have described in detail the phase precipitation phenomenon, and tried to sort out the driving factors. In the next section, we would like to discuss the changes of macromolecule conformation and the aggregation process, through viscosity and light scattering measurements. Finally, a quantitative explanation of such phenomena requires the knowledge of the constant of the ion-polyion association and of the nature of the complex. We will discuss in the last part the results of conductimetric and densimetric measurements.

Chain conformation and aggregation

Viscosity. In the first series of experiments, the reduced viscosity, η_{red} , of the polymer solutions at constant C_p was measured, as a function of the CaCl₂ concentration, at 25°C. These measurements were made using a capillary viscosimeter. In fact, these solutions of strongly expanded high molecular weight polymers are non-newtonian. Then the data correspond to the shear-thinning regime, and can be only qualitatively discussed and used with an aim of comparison of the various polymers.

In the range of the lower CaCl₂ concentration ($C_s < C_s^*$), comparative measurements of AD and H polymers confirm the differences observed according to the method of preparation. *Figure 7* shows indeed that η_{red} of H3 solutions is higher than that of AD60 solutions, at low C_s . We have also observed that this gap decreases when τ decreases.

In a more extended range of C_s , up to C_s^{**} , η_{red} passes through a minimum for all the samples (*Figure 8*). This result is consistent with the resolubilization behaviour discussed above. Curves exhibiting a minimum are observed for the lower value of τ as well, when phase separation does not occur at 25°C, meaning that the polymer conformation changes in the same way even in the absence of precipitation.

In a second series of experiments, the low shear viscosity was measured at constant concentrations of NaCl and CaCl₂ as a function of C_p . The variations of $\eta_{red} = f(C_p)$ were found to be linear. The values of the intrinsic viscosity $[\eta]$ and of the Huggins constant, K' , are reported in *Table 3*. Let us note that we varied the ξ parameter by changing either τ (various AD samples) or α (AD60 sample). K' ranges from 0.35 to 0.55 with NaCl, while it increases from 1 to 1.8 when CaCl₂ concentration increases. This clearly indicates the formation of aggregates in the presence of Ca²⁺ cations through intermolecular bridges. Since this aggregation

phenomenon must disappear when the polymer concentration is low enough to make the bridge formation improbable, one could expect that even in the presence of Ca^{2+} , the values of η_{red} extrapolated at $C_p = 0$ represent the conformation of the isolated polymer coil in interaction with these cations.

Light scattering and viscosimetry experiments on variably ionized acrylamide/sodium acrylate copolymers, made by Reed *et al.*⁴⁹, yielded apparent electrostatic persistence lengths and intrinsic viscosity varying both as the inverse square root of the ionic strength $I^{-0.5}$ and linearly with ξ . In the limit of zero polymer concentration, the equivalent hydrodynamic radius R_H was found to be independent of ionic strength, whereas the radius of gyration, $\langle S^2 \rangle^{1/2}$, varied strongly according to the following expression:

$$\langle S^2 \rangle^{1/2} - \langle S^2 \rangle_0^{1/2} = [(Mb/3m)(350\xi/I^{0.5})]^{1/2} \quad (2)$$

where M is the molecular weight of the polymer, $m = 71$ is the mass of monomer and $b = 2.56 \text{ \AA}$ is the contour distance between monomers. $\langle S^2 \rangle_0^{1/2}$ is the radius of gyration of the homologue non-hydrolysed polymer (polyacrylamide), and I is the ionic strength of the solution, calculated from:

$$I = \sum \frac{z^2}{2} [M] + \frac{C_{\text{ip}}}{2} \quad (3)$$

where $[M]$ is the molar concentration of each ion M , and z its charge. $[\eta]$ was therefore found to be a linear function of $\langle S^2 \rangle$ by Reed *et al.*⁴⁹, but the curves corresponding to the different AD did not superimpose well.

The plots (not shown) of $([\eta] - [\eta]_0)$ vs $\xi/I^{1/2}$, for both the NaCl and CaCl_2 are linear. $[\eta]_0$ is the intrinsic viscosity of the nonhydrolysed polyacrylamide of the same molecular weight $[\eta]_0 = 1000 \text{ ml g}^{-1}$, calculated from the expression of François *et al.*⁵⁰,

$$[\eta]_0 = 9.3 \times 10^{-3} M_w^{0.75} (\text{ml g}^{-1}) \quad (4)$$

The linearity of the function is verified but the slopes A of the curves are higher in presence of NaCl than with CaCl_2 and decrease in both cases when the charge parameter ξ increases as:

$$[\eta] - [\eta]_0 = A\xi I^{-1/2} \quad (5)$$

The fact that the curves are not superimposed indicates that ξ and I are not the only parameters which affect the ion-polyion interactions. Moreover, all the curves extrapolate at $[\eta] - [\eta]_0 = 0$, constituting a further argument to think that $[\eta]$ reflects the conformation of the isolated coil.

Kowblanski and Zema⁵¹ measured the activity coefficients γ for Na^+ ions, in partially hydrolysed polyacrylamide solutions, varying ξ parameter, at ionization degree $\alpha = 1$. Neither the Manning^{35,36} nor Iwasa and Kwak⁵² theory adequately described the behaviour of counterions over the entire range of charge densities they investigated. Such approaches predict an abrupt change in the variation of γ with ξ when $\xi = \xi_c$, ξ_c being a critical value above which condensation of the counter ions on the polymer takes place. The values of ξ_c are 1 and 0.5 for monovalent and divalent counter ions respectively. Kowblanski and Zema⁵¹ observed a strong decrease of γ when ξ increases even for $\xi < \xi_c$ and suggested that condensation occurs

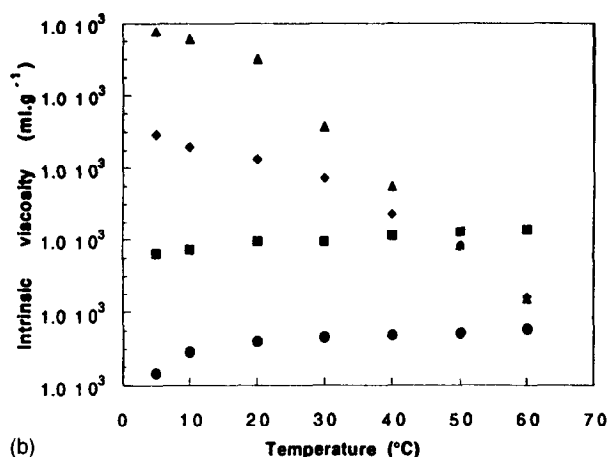
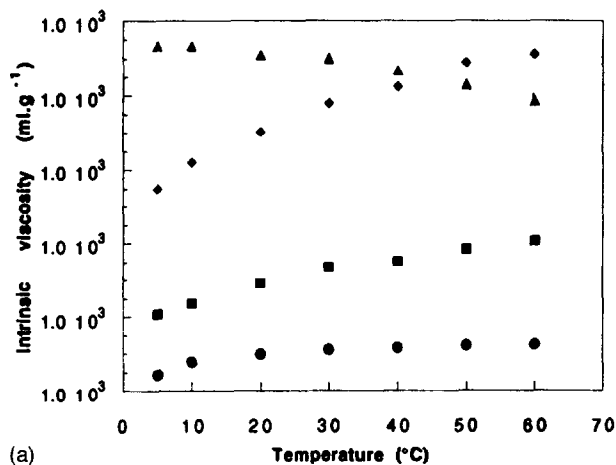


Figure 9 Temperature dependence of the low shear intrinsic viscosity in the presence of 0.25 mol l^{-1} NaCl (a) and 0.04 mol l^{-1} CaCl_2 (b) for: AD10 (●); AD17 (■); AD37 (◆); AD60 (▲)

below as well as above ξ_c . An empirical linear relationship between the square root of the polyelectrolyte charge density and the measured counterion activity coefficients was demonstrated by these authors, to hold over both sides of ξ_c , the Manning's critical charge parameter defined as $|z|^{-1}$. They gave the following relations for Na^+ and Ca^{2+} ion activity coefficients respectively^{51,53}:

$$\gamma_{\text{Na}^+} = (0.96 - 0.42\xi^{1/2}) \quad (6)$$

$$\gamma_{\text{Ca}^{2+}} = (0.43 - 0.26\xi^{1/2}) \quad (7)$$

The plot (not shown) of the slopes A (equation (5)), vs the activity coefficient, using γ_i values calculated from equations (6) and (7) for Na^+ and Ca^{2+} ions respectively indicates that the A parameter increases linearly with the activity coefficients and, interestingly enough, the relations are the same for sodium and calcium ions.

Starting from this idea of ion condensation, Kowblanski and Zema⁵⁴ demonstrated a semi-empirical law for the variation of $[\eta]$ for the partially hydrolysed polyacrylamide in the presence of NaCl, expressed as:

$$[\eta] = [\eta]_0 + k\xi\gamma_{\text{Na}^+} \quad (8)$$

The term $k\xi$ is viewed as the viscosity due to the hypothetical maximum electrostatic expansion of the polyion of charge density ξ in the absence of any counterion-polyion interactions. Replacing in equation

(8) γNa^+ by its expression (6), gives a term $0.42 k\xi^{3/2}$, which represents the reduction of $k\xi$ due to interaction of the polyion with its monovalent counterions. Kowblansky and Zema⁵⁴ obtained linear correlation, going through the origin, for $([\eta] - [\eta]_0)/\gamma\text{Na}^+$ versus ξ . The values of k , determined as the slopes of these plots, were shown by these authors, to linearly increase with the inverse square root of the simple salt concentration, establishing therefore an expression similar to the one derived in our case:

$$[\eta] - [\eta]_0 = k'\xi\gamma I^{-1/2} \quad (9)$$

The constant k' we obtain is equal to 2743 ml g^{-1} , including calcium ions. The value obtained by Kowblansky *et al.* is 690 ml g^{-1} for sodium ions alone, but for polymers of smaller molecular weight (1.5×10). Indeed, to generalize expression (9), the molecular mass must be taken into account:

$$[\eta] - [\eta]_0 = C^{\text{st}} M \cdot \xi\gamma I^{-1/2} \quad (10)$$

The results of Kulkarni and Gundiah^{55,56} reported together with the data obtained by Kowblansky and Zema⁵⁴, Schwartz and François⁵⁷, Truong⁵⁸ and Kheradmand⁵⁹ show that the slope k' varies linearly with the molecular weight (figure not shown).

Figure 9 shows the variations of intrinsic viscosity as a function of temperature for AD 10, 17, 37 and 60, sodium salt polymers in presence of 0.25 M NaCl (Figure 9a) or 0.04 M CaCl_2 (Figure 9b), at pH 8. $[\eta]$ increases with the temperature for low values of τ (< 0.17) in both cases of added salts; for high values of τ (> 0.17) the intrinsic viscosity decreases when temperature increases, in the presence of calcium. For the lower charge parameters, this behaviour is in fact reminiscent of that described for the unhydrolysed polyacrylamide. It was indeed shown that the θ point of the PAM in aqueous solution is about -8°C , which means that the second virial coefficient and the macromolecular dimensions are increasing functions of the temperature⁵⁰. Therefore, we can assume that the temperature dependence of the viscosity of the hydrolysed polymers is due to two antagonistic effects: the increase of solvent quality with respect to the non ionic part of the chain and the decrease of the virial associated with the ionic part and due to the cation binding. For the lower values of τ , the first effect dominates, while the second one becomes preponderant for the higher charge parameters. These results are consistent with the turbidity measurements which show that the polymer stability decreases with the temperature. The potentiometric results obtained by Rinaudo and Milas⁶⁰ for carboxymethyl-cellulose in the presence of calcium, also indicated an increase of Ca^{2+} fixation when the temperature increased.

These viscosimetric investigations lead to the following important conclusions:

- As expected from the solubility studies, the interactions between the calcium ions and the polyions are stronger when the distribution of the charges tends to be sequential, as in copolymers AD. This effect affects the viscosity.
- The resolubilization at high CaCl_2 concentration is correlated with an increase of the reduced viscosity.
- The intrinsic viscosity determined by extrapolation of η_{red} at $C_p = 0$ reflects probably the conformation of the isolated coils and its variation with ξ and I can be

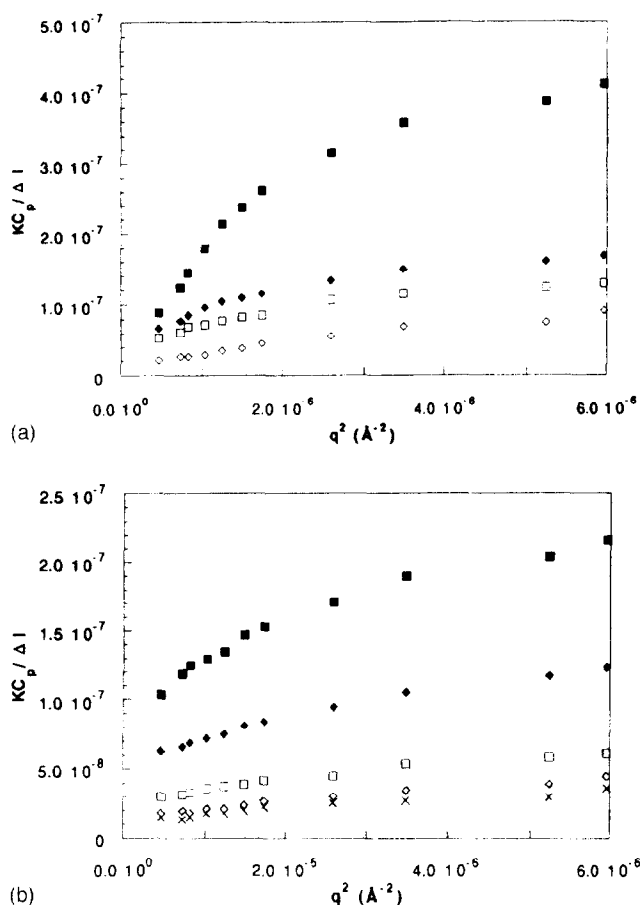


Figure 10 Light scattering: changes of $KC_p/\Delta I = f(q^2)$ as a function of the time (t) after addition of CaCl_2 (0.024 mol l^{-1}) for AD60 at $C_p = 0.1 \text{ g l}^{-1}$: (a) $T = 25^\circ\text{C}$; (b) $T = 40^\circ\text{C}$

directly related to a degree of cation binding expressed through the activity coefficient of these cations.

- The viscosity sharply drops in the presence of calcium, in agreement with the loss of solubility.
- The Huggins constant is much higher in the presence of calcium than with sodium. This suggests the presence of swelled aggregates and the following light scattering experiments were made to verify this assumption.

Light scattering. Light scattering experiments were carried out under the same conditions as the viscosity measurements, in the presence of NaCl and CaCl_2 .

For NaCl, the results confirm the variations of the radius of gyration versus $\xi \cdot I^{-0.5}$ (relation (2)).

In the case of CaCl_2 two different behaviours were observed. For the AD sample of lower degree of hydrolysis, a classical Zimm plot was obtained with an almost linear dependence of $KC_p/\Delta I$ as a function of the square scattering vector q^2 (K is an optical constant and ΔI is the difference between the scattered intensity of the solution and that of the solvent). In this case (AD17) the slope of the curves $KC_p/\Delta I = f(q^2)$ decreases when CaCl_2 is added in the solutions, while the extrapolation at $q = 0$ does not vary with C_s . This means that CaCl_2 induces the collapse of the chains, but does not provoke their aggregation.

On the contrary, for the higher degree of hydrolysis the light scattering results clearly demonstrate the formation of particles of high molecular weight. Figures

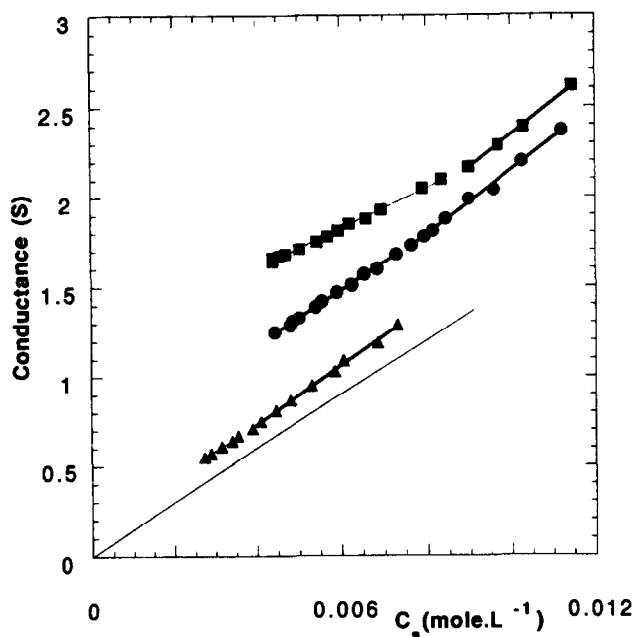


Figure 11 Variation of the conductance of the AD60 solutions as a function of CaCl_2 concentration: $C_p = 10^{-3} \text{ g ml}^{-1}$ (\blacktriangle); $C_p = 3 \times 10^{-3} \text{ g ml}^{-1}$ (\bullet); $C_p = 10^{-3} \text{ g ml}^{-1}$ (\blacksquare)

10a and 10b show the evolution of $KC_p/\Delta I = f(q^2)$ as a function of time for the AD60 sample ($C_p = 10^{-4} \text{ g ml}^{-1}$) after addition of CaCl_2 (0.024 M), at two different temperatures. Very soon after the addition of CaCl_2 , the downward curvature of the q^2 dependencies of the scattered intensity indicates the presence of polydisperse aggregates. At time greater than 960 min, at 25°C , the scattered intensity changes no more, the angular dependence becoming linear. At equilibrium, the average molar mass of the particles is $(60 \pm 10) \times 10^6$ (approximately ten times the initial molecular weight) and $(100 \pm 20) \times 10^6$ at 25°C and 40°C respectively. The average radius of gyration reaches values of the order of $6000 \pm 1000 \text{ \AA}$ at 25°C but of only $1400 \pm 200 \text{ \AA}$ at 40°C . These values are approximate, since the data correspond to values of q out of the Guinier range, and the development of the $P(q)$ function $P(q) = 1 + q^2 \langle S^2 \rangle / 2$ has to be used. These results are in agreement with the viscosimetric behaviour. One may assume that aggregates of almost the same molecular weight are formed when concentration increases at each temperature, while these dimensions are much lower at higher temperatures.

Ion-polyion interactions

Conductimetry. Conductimetry can be used in order to detect a strong interaction between ions and polyions, since the binding of the cations is expected to result in a loss of conductivity.

Figure 11 allows us to compare the variations of the specific conductivity κ as a function of CaCl_2 concentration in the absence and in the presence of sample AD60. In polymer free solutions, the curve is almost linear, and its slope, P_0 , is approximately equal to the sum of the equivalent conductivities of Ca^{2+} and Cl^- . In the presence of AD60, two regions can be distinguished:

(a) $C_s < C'_s$ where the slope P is significantly lower than P_0 . This corresponds to the binding step,

Table 4 Values of critical salt concentrations (C_s^*), calculated fractions of Ca^{2+} bound to the polymer (m) and carboxylate groups linked to a Ca^{2+} (f), as determined by conductimetry for the AD60 and 37 samples, at various polymer concentrations. In the last column, are given the values of the association constant deduced from these results

Sample	C_p	C_{ip}	C_s^*	C'_s	m	f	K_b
AD60	1.1	5.4	15	3.4	0.37	0.47	7.8×10^4
	2.2	10.6	13	3.6	—	—	—
	3.3	16.3	11	7.5	0.46	0.43	1×10^4
	4.1	20.3	11	8.5	0.55	0.46	1.2×10^4
	5	24.7	12	9	0.67	0.49	1.2×10^4
AD37	3.3	11.1	20	5.5	0.28	0.28	6.2×10^3
	4.0	13.9	16	6	0.32	0.28	5×10^3
	8.6	29.7	19	6.25	0.71	0.30	6×10^3

(b) $C_s > C'_s$, where the slope recovers the value of P_0 . The breakdown of the cure is generally attributed to the saturation of the polymer by the cations.

Table 4 shows that C'_s is significantly lower than C_s^* when C_p and τ are low. This means that the phase separation occurs for salt concentrations higher than that required for the polymer saturation under these conditions while for the higher C_p and τ , the two phenomena coincide. The slope obtained for $C_s < C'_s$ decreases when C_p increases. This indicates that a part of the cations Ca^{2+} are bound by the polymer, and suggests that this fixation is ruled by an equilibrium law. The ion binding is not surprising for AD60, since the value of the Manning charge parameter^{35,36} ($\xi = 1.01$) is much higher than the critical threshold of divalent cation condensation, $\xi_c = 0.5$.

However, the Ca^{2+} binding appears even for sample AD27 of $\xi = 0.49$. One must conclude that the precipitation of these polymers is due at least partially to a cation binding, despite their relatively low charge parameter. This observation is consistent with the results of Kowblansky and Zema^{51,53}, who have shown that the activity coefficients of Na^+ and Ca^{2+} in the aqueous solutions of polymers of type H are much lower than those predicted by Manning. The presence of charged sequences along the chain may explain the discrepancies between the experiments and theories which consider the polyelectrolyte as a uniformly charged line. As a matter of fact, these conductivity measurements confirm the role played by the ionic binding in the precipitation of these polymers.

Using simple arguments developed by Ikegami and Imai⁵, it is possible to obtain an order of magnitude of the fraction of Ca^{2+} ions bound by the polymer ($m = C_{\text{sbound}}/C_s$) from the ratio P/P_0 ; for $C_s < C'_s$:

$$\frac{P}{P_0} = 1 - m \frac{\frac{1}{2} \lambda_{\text{Ca}^{2+}} + \lambda_p}{\frac{1}{2} \lambda_{\text{Ca}^{2+}} + \lambda_{\text{Cl}^-}} \quad (11)$$

where λ_p , $\lambda_{\text{Ca}^{2+}}$ and λ_{Cl^-} are the equivalent conductivities per charge of the polyanion, per Ca^{2+} and per Cl^- respectively. Some results are gathered in Table 4. Parameter m increases when C_p and τ increase and always remains lower than unity. Ikegami and Imai have found $m = 1$ for PAA. From the values of m , the fraction, f , of carboxylate groups which are bound to a Ca^{2+} ion can also be estimated. In Table 4, the values of f obtained for $C_s = C'_s$ are given. f is also lower than 1, and since the polymer is assumed to be saturated for $C_s > C'_s$, this means that phase separation occurs when

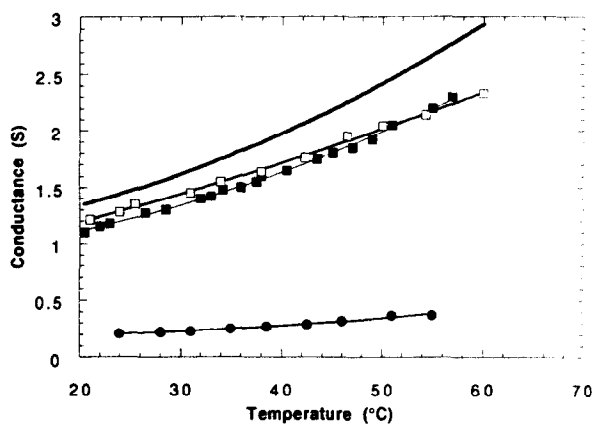


Figure 12 Temperature dependencies of the conductance of a solution of AD60 ($C_p = 10^{-3} \text{ g ml}^{-1}$) (●), of a solution of CaCl_2 ($C_s = 10^{-2} \text{ mol l}^{-1}$) (■), and of a solution containing $10^{-3} \text{ g ml}^{-1}$ of AD60 and $10^{-2} \text{ mol l}^{-1}$ (□). The upper curve is calculated, by assuming the additivity of the conductivities of the polymer and of CaCl_2 : $A + B$

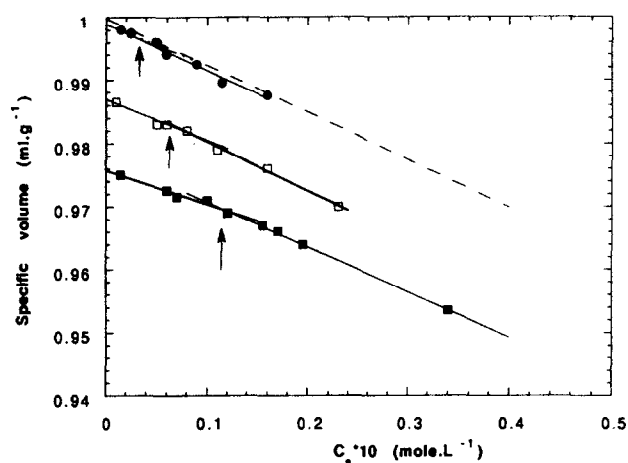


Figure 13 Variation of the specific volume of solutions of AD60 as a function of the concentration of CaCl_2 : $C_p = 0$ (---); $C_p = 7 \times 10^{-4} \text{ g ml}^{-1}$ (●); $C_p = 4 \times 10^{-3} \text{ g ml}^{-1}$ (□); $C_p = 4 \times 10^{-3} \text{ g ml}^{-1}$ (■). The arrows indicate the values of C_s''

the carboxylate groups are not all neutralized. As discussed later, these measurements allow us to determine an order of magnitude of the binding constant.

Figure 12 shows the temperature dependencies of κ of a CaCl_2 solution (concentration c_a), of a AD60 solution (concentration C_p) and for a mixture containing polymer and salt at concentration C_p and C_s respectively. Besides, the upper curve in this figure was calculated for the mixture by assuming the additivity of the contribution to the conductivity of each component. The experimental curve lies below the calculated one and its slope is significantly lower. This result reveals an enhancing of the binding by heating, and is consistent with the loss of solubility at high temperature.

Densimetry. Densimetry has been applied with success in the past^{8,61-62} to the study of the ion-polyion interactions, because it allows precise characterization of the perturbations in the hydration shell of the ionic species associated with the binding. Indeed, if the additivity of the partial specific volumes of each constituent is assumed, the specific volumes v_1 and v_2 of a polymer

solution free of salt (CaCl_2) (expression (12)) and of a polymer solution with added salt (expression (13)) respectively, one can write:

$$v_1 = w_e v_e + w_s v_s \quad (12)$$

$$v_2 = w_e F v_e + w_s F v_s + w_p v_p \quad (13)$$

with
$$F = \frac{w_s + w_e}{w_s + w_e + w_p} \quad (14)$$

w_e and w_s are the concentrations in g g^{-1} of water and salt in solution (12), w_p is the concentration in g g^{-1} of polymer in solution (13), and v_e , v_s and v_p are the specific volumes of water, salt and polymer respectively. If the additivity is not verified, the measured specific volume (12), v_3 , will differ from v_2 and the slope of $v_3 = f(w_s)$ will be lower than that of $v_2 = f(w_s)$ (in absolute value). The discrepancy can be related to the number n of hydration molecules released when ion binding occurs.

$$v_3 - v_2 = \frac{nmw_s M_e (v_e - v_h)}{M_s} \quad (15)$$

v_h is the partial specific volume of water molecules inside the hydration shell, lower than v_e . A positive value of $v_3 - v_2$ indicates a release of some hydration molecules. Moreover, if the difference, $v_e - v_h$ (0.36 ml mol^{-1} for Ca^{2+}) and m are known, it is possible to determine n . A value of $n = 6$ has been obtained for sodium acrylate in the presence of CaCl_2 , which means that this cation loses its hydration shell⁶².

The variations of v_3 are reported in Figure 13 for the different polymer concentrations, and can be compared with the variation of v_1 . Relations (12) and (13) show that, in the absence of interactions, the slopes of v_2 and v_1 must be equal. The results can be rationalized by distinguishing two different parts in the curves: for $C_s < C_s''$ and $C_s > C_s''$ where the absolute values of the slopes of v_3 are lower, and equal to that of v_1 , respectively. The values of C_s'' should be in agreement with the values of C_s' , measured by conductimetry (see above), since the water release is only expected in the concentration range where the binding occurs. Nevertheless, the effects measured by densimetry are very small and, for AD60, the estimated number of released water molecules is about three, to be compared with six in the case of PAA. Moreover, n decreases when τ decreases, and, interestingly enough, the value of n found for the H3 sample is 1, which confirms the weaker interactions of the hydrolysis products with Ca^{2+} .

DISCUSSION

Our experimental results stressed the fact that the phase separation of acrylamide-acrylic acid copolymers or hydrolysed polyacrylamides in the presence of divalent cation salts do not obey the general laws described in the literature.

The critical salt concentrations C_s^* , at the threshold of precipitation are lower than those predicted by the H type model; they are a function of polymer concentration, and increase with temperature and when the salt concentration increases. However, for some values of the polymer concentration, hydrolysis ratio and temperature, the C_s^* values are higher than the values corresponding to the stoichiometry of the L type precipitation model.

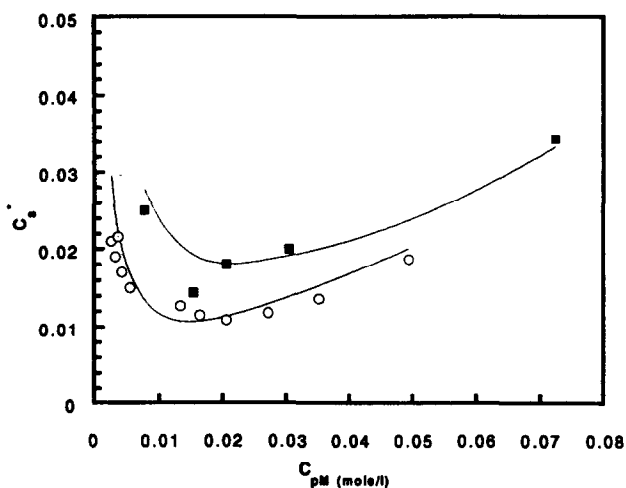


Figure 14 Fits of the solubility limits with equation (16) for AD37 (○) and AD27 (■)

In short, our results show that there is a shift from the H type to the L type of behaviour when one of the following parameters increases: the polymer concentration; the added monovalent salt; the hydrolysis ratio; the temperature. This shift is also observed when the fraction of triad sequences of carboxylate groups increases in the backbone of the polymer.

We would like to propose an attempt to explain the phase diagram from a simple approach.

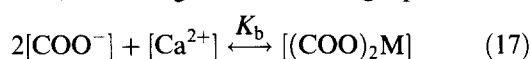
Phase diagrams

The systems obtained by the interactions between ions and polyions may be outlined, as already proposed³³, by writing the free energy as a sum of three terms due to the contributions of the uncharged units (acrylamide units in this case), the ionized units (dissociated acrylate units) and the acrylic acids units neutralized by the divalent cation (COO_2Ca). Under our experimental conditions, we can neglect the units bearing acid function (COOH). The fraction of neutral units is $(1 - \tau)$, and several studies on the polyacrylamide suggest that their contribution to the second virial coefficient in water is positive⁴⁹. The fraction of ionized units is $\tau(1 - f)$, where f is the fraction of carboxylate functions complexed by a divalent cation and their contribution to the virial is positive and proportional to $1/I$, I being the ionic strength of the medium. Finally, the virial associated to the complexed units is assumed to be strongly negative. Then, a given fraction f^* of these units is required to minimize the free energy and get the phase separation. Axelos *et al.*³³ have demonstrated that the following relation can be obtained between c_s^* and f^* , C_{ip} (or τC_p)

$$C_s^* = \frac{f^* C_{ip}}{2} + \frac{f^*}{2K_b C_{ip} (1 - f^*)^2} \quad (16)$$

Such an expression is based upon some approximations:

- The pH is high and the ionization equilibrium of the carboxylate functions can be neglected. The phase diagrams of Figure 3 were established under these conditions.
- The interactions between the carboxylate groups and the divalent cations lead only to the formation of bicomplexes, according to the following equilibrium:



- The polyelectrolyte effect is neglected since the charges are assumed to be uniformly distributed in the bulk. It has been shown that such an hypothesis is reasonable for polymer concentrations higher than the overlapping critical concentration (in the semi dilute regime)^{11-13,16,17}.

Equation (16) means that for a strongly charged polymer and/or for a high value of the complexation constant, C_s^* must be a linear function of C_{ip} , since the second term vanishes. This corresponds to the phase separation of type L. For lower values of K_b or τ , C_s^* will be a decreasing function of C_{ip} at low c_{pM} (second term predominant) and becomes an increasing linear function of C_{pM} at higher C_{ip} (first term predominant). Then a minimum of C_s^* vs C_{ip} is expected as observed in the cases of copolymers of the AD series. Figure 14 shows that equation (16) indeed allows us to fit quite well the solubility limit of AD60 and AD37, with $K_b = 8 \times 10^4$, $f^* = 0.85$ and $K_b = 10^5$, $f^* = 0.95$ respectively. The value of f^* is higher for AD37 than for AD60, which is consistent with our hypothesis, the positive contribution of the acrylamide units preventing precipitation. Thus, this simple model seems to be able to give a rather good account of the phase separation phenomenon with calcium ions at room temperature and in the absence of other salts.

From this model, it is also possible to understand at least qualitatively several behaviours described above.

The equilibrium constant K_b may be written as:

$$K_b = K_{b0} \exp(-3\kappa l_B) \exp\left(-\frac{\Delta H_0}{T}\right) \quad (18)$$

where l_B is the Bjerrum length and K^2 is the screening length:

$$\kappa^2 = 4\pi l_B \left(C_{ip}(2 - f) + C_{\text{NaCl}} + 2C_s + 4\left(c_s - \frac{fC_{ip}}{2}\right) \right) \quad (19)$$

The introduction of the screening length in the complexation constant expresses the fact that interactions between divalent ions and polyions are screened out at high ionic strength³². This well explains why a resolubilization of the polymer is observed when a large excess of CaCl_2 or NaCl is added to the system. For a high enough screening length, the critical amount of complexes cannot be reached and the polymer remains soluble.

Equation (19) is also of the Arrhenius type, and if the activation energy ΔH_0 is positive, the complexation will be favoured by heating. If the critical value f^* is not temperature dependent, its value is reached for a lower concentration of divalent cations when T increases, and the phase separation must occur sooner. The thermal effect on the polymer stability can be simply explained in this way, and this is consistent with the results of the conductivity as a function of temperature.

It must be pointed out that we consider the virial of the neutral units as varying slightly with different parameters, which is probably not correct. Moreover, only formation of bicomplexes are taken into account, while in other theoretical work³², the formation of mono-nuclear complex is also considered. In this respect, it is interesting to remark that the behaviour of the copolymers of the H series cannot be explained by our

oversimplified model. Indeed, equation (16) cannot fit the solubility limits shown in *Figure 3* obtained with polymers of the H series. Let us remember that the main difference between the two series of polymers consists in the distribution of the acrylic units. Then, the formation of bicomplexes may be favoured by the high fraction of carboxylate diads in the case of copolymers of the AD series, while in the H series, where the carboxylate tend to be isolated, mainly monocomplexes may be formed. However, we did not get satisfactory results, by applying to our systems the theory of Wittmer *et al.*³², which considers the monocomplexes.

Finally, it was interesting to compare the values of K_b which allows us to fit the solubility limits with equation (16) and those which can be deduced from the conductivity measurements (*Table 4*). If one value obtained for AD60 at the lower polymer concentration is excepted, conductivity leads to lower K_b values. This gives the limits of our model. Indeed, the hypothesis according to which f^* is constant is equivalent to considering that practically all the divalent cations added in the solution are bound by the polymer up to its saturation, which corresponds to a very high K_b constant. Then, none of them can contribute to increasing the ionic strength of the medium, and consequently lower the virial associated with the remaining charged monomers. If this is not the case, the f^* value must decrease continuously with the C_s , since a lower fraction of complexed units will be necessary to get a zero value for the virial coefficient. Moreover, the anions of the divalent salt also have an ionic strength effect, which is not taken into account in our model.

CONCLUSION

This work gives a lot of information on the behaviour of acrylamide and acrylic acid copolymers in aqueous solution in the presence of alkaline earth cations. The phase diagrams were established under various conditions of temperature and ionic strength. One of the most interesting features of these diagrams consists of the existence of two-phase separation limits at low and high salt concentrations. This behaviour is comparable with that obtained by adding an excess of monovalent salt with respect to the divalent one. The whole set of results concerning this precipitation phenomenon can be roughly understood through a rude model based on a simple calculation of the free energy of the system, and assuming that the polyion-ion interactions mainly result in the formation of a bicomplex. Nevertheless, some differences between the constant of formation of the complexes, which allows a fit of the solubility limits, and those obtained more directly by conductivity measurements illustrate the limits of our oversimplified model. Moreover the interesting role played by the distribution of the monomers units along the chain is not taken into account.

Besides, the variation of the chain dimension in the limit of zero concentration were studied by viscosimetry. A universal law was obtained, sodium and calcium ions introducing a term of counterion activity determined by Kowblansky and Zema. At higher concentrations, the addition of divalent cations provokes the formation of large aggregates.

REFERENCES

- Mandel, M., in *Polymer Science and Engineering*, 2nd Edn, ed. H. F. Mark, M. Bikales, C. G. Overberger and G. Mendès. John Wiley, New York, 1985.
- Armstrong, R. W. and Strauss, U. P., in *Encyclopedia of Polymer Science and Technology*, Vol. 10, ed. H. F. Mark, N. G. Gaylord, N. M. Bikales. Wiley-Interscience, New York, 1969, p. 781.
- Strauss, U. P. and Ander, P., *J. Am. Chem. Soc.*, 1958, **80**, 6494.
- Fisenberg, H. and Woodsid, D., *J. Chem. Phys.*, 1962, **36**, 1844.
- Ikegami, A. and Imai, N., *J. Polym. Sci.*, 1962, **56**, 133.
- Michaeli, I., *J. Polym. Sci.*, 1960, **48**, 291.
- Strauss, U. P. and Siegel, A. J., *J. Phys. Chem.*, 1963, **67**, 2683.
- Strauss, U. P. and Leung, Y. P., *J. Am. Chem. Soc.*, 1965, **87**, 1476.
- Flory, P. J., *J. Chem. Phys.*, 1953, **21**, 162.
- Buscall, R. and Corner, T., *Eur. Polym. J.*, 1982, **18**, 967.
- Rabhari, R. and François, J., *Polymer*, 1988, **29**, 851.
- Rabhari, R. and François, J., *Polymer*, 1992, **33**, 1449.
- Rabhari, R. and François, J., *Polymer*, 1988, **29**, 845.
- El Brahmi, K., Ph.D. thesis, University Louis Pasteur, Strasbourg, 1991.
- El Brahmi, K., François, J. and Dupuis, D., *Rheologica Acta*, 1995, **34**, 1, 86.
- Allain, C. and Salomé, L., *Macromolecules*, 1990, **23**, 981.
- Allain, C. and Salomé, L., *Polymer Communications*, 1987, **28**, 109.
- Burrafato, G. *et al.*, *Macromolecules*, 1990, **23**, 2402.
- Garnier, C., Axelos, M. A. V. and Thibault, J. F., *Carbohydr. Res.*, 1993, **240**, 219.
- Garnier, C., Ph.D. thesis, Université de Nantes, 1992.
- Schwartz, T. and François, J., *Makromol. Chem.*, 1981, **182**, 2775.
- Truong, N. D., Galin, J. C., François, J. and Pham, Q. T., *Polymer Communications*, 1984, **25**, 208.
- Truong, N. D. and François, J., in *Solid-Liquid Interactions in Porous Media*, Vol. 42, Technip, Paris, 1985, p. 251.
- Mestdagh, M. M., Want, L., Velings, N. and François, J., *Polymer*, to be published.
- Truong, N. D., Galin, J. C., François, J. and Pham, Q. T., *Polymer*, 1986, **27**, 459, 467.
- Panzer, H. P. and Halverson, F., *Proceedings of the Engineering Foundation Conference*, Palm Coast, Florida, 1988, 239.
- Higuchi, M. and Senju, R., *Polymer*, 1972, **3**, 370.
- Sawant, S. and Morawetz, H., *Macromolecules*, 1984, **17**, 2427.
- Kheradmand, H., François, J. and Plazanet, V., *Polymer*, 1988, **29**, 860.
- Delsanti, M., Dalbicz, J. P., Spalla, O., Belloni, L. and Drifford, M., *Macro Anion Characterization from Dilute Solutions to Complex Fluids*, ed. K. S. Schmitz. ACS, Washington DC, 1994.
- Olivera de la Cruz, O., Belloni, L., Delsanti, M., Dalbicz, J. P., Spalla, O. and Drifford, M. J., *J. Chem. Phys.*, 1995, **103**, 1.
- Wittmer, J., Johner, A. and Joanny, J. F., *J. Phys. (Paris)*, 1993, **II,5**, 6335.
- Axelos, M., Mestdagh, M. M. and François, J., *Macromolecules*, 1994, **27**, 6594.
- Boutin, J. and Contat, S., *French Patent No. 2495217*, issued from Rhône Poulenc Ind.
- Manning, G. S., *J. Chem. Phys.*, 1969, **51**, 924.
- Manning, G. S., *Rev. Biophys.*, 1978, **11**, 179.
- Gramain, P. and Libeyre, R., *J. Appl. Polym. Sci.*, 1970, **14**, 383.
- Sarazin, D., Le Moigne, J. and François, J., *J. Appl. Polym. Sci.*, 1978, **22**, 1377.
- Libeyre, R., Sarazin, D. and François, J., *Polym. Bull. (Berlin)*, 1981, **4**, 53.
- Zaitoun, A. and Potié, B., *IFP report*, 1982, ref. 30348.
- Kagawa, I. and Fuoss, R. M., *J. Polym. Sci.*, 1995, **18**, 535.
- Mandel, M. and Leyte, J. C., *J. Polym. Sci.*, 1964, **A2**, 2883.
- Mandel, M. and Jenard, A., *Trans. Faraday Soc.*, 1963, **59**, 2170.
- Cabaness, W. R., Yen-Chin-lin, T. and Paranyl, C., *J. Polym. Sci.*, 1971, **A1,9**, 2155.
- Pontratan, S. and Kapur, S. L., *Makromol. Chem.*, 1977, **178**, 1029.
- Truong, N. D., Medjahdi, G., Sarazin, D. and François, J., *Polym. Bull. (Berlin)*, 1990, **24**, 101.
- El Brahmi, K., Rawiso, M. and François, J., *Eur. Polym. J.*, 1993, **29**, 1531.
- Mahi, A. and François, J., unpublished results.

49. Reed, W. F., Ghosh, S., Medjahdi, G. and François, J., *Macromolecules*, 1991, **24**, 6189.
50. François, J., Schwartz, T. and Weill, G., *Macromolecules*, 1980, **13**, 564.
51. Koblansky, M. and Zema, P., *Macromolecules*, 1981, **14**, 166.
52. Iwasa, K. and Kwak, J. C. T., *J. Chem. Phys.*, 1997, **81**, 408.
53. Koblansky, M. and Zema, P., *Macromolecules*, 1981, **14**, 1451.
54. Koblansky, M. and Zema, P., *Macromolecules*, 1981, **14**, 1448.
55. Kulkarni, R. A. and Gundiah, S., *Makromol. Chem.*, 1984, **185**, 957.
56. Kulkarni, R. A. and Gundiah, S., *Makromol. Chem.*, 1984, **185**, 969.
57. Schwartz, T. and François, J., *Makromol. Chem.*, 1981, **182**, 2757.
58. Truong, N. D., Ph.D. thesis, Université Louis Pasteur, Strasbourg, 1984.
59. Kheradmand H., Ph.D. thesis, Université Louis Pasteur, Strasbourg, 1987.
60. Rinaudo, M. and Milas, M., *Macromolecules*, 1973, **6**, 879.
61. Begala, A. J. and Strauss, U. P., *J. Phys. Chem.*, 1972, **76**, 3451.
62. Tondre, C. and Zana, R., *J. Phys. Chem.*, 1972, **76**, 23.